Exchange Coupling in Cyano-Bridged Homodinuclear Cu(II) and Ni(II) Complexes: Synthesis, Structure, Magnetism, and Density Functional Theoretical Study

Antonio Rodríguez-Fortea, Pere Alemany,* Santiago Alvarez, and Eliseo Ruiz*

Departament de Química Inorgànica, Departament de Química Física, and Centre de Recerca en Química Teòrica (CeRQT), Universitat de Barcelona, Diagonal 647, 08028 Barcelona, Spain

Ariane Scuiller, Caroline Decroix, Valérie Marvaud,* Jacqueline Vaissermann, and Michel Verdaguer*

Laboratoire de Chimie Inorganique et Matériaux Moléculaires, CNRS 7071, Université Pierre et Marie Curie, F-75252 Paris Cedex 05, France

Izio Rosenman

Groupe de Physique des Solides, Université Denis Diderot, F-75252 Paris Cedex 05, France

Miguel Julve

Departament de Química Inorgànica, Facultat de Química, Universitat de València, Dr. Moliner 50, 46100 Burjassot, València, Spain

Received December 18, 2000

The synthesis and structural characterization of several new cyano-bridged copper(II) and nickel(II) homodinuclear complexes is presented. The measure of magnetic properties for these complexes is complemented with a computational study of the exchange coupling for several model structures representing this family of compounds. The influence of several factors on the coupling constant has been examined, coordination position occupied by the bridging ligand, distortions of the coordination environment, and relative disposition of the cyanide ion with respect to the M−M vector. Comparison of experimental and calculated coupling constants allows for the rationalization of the most relevant features of the exchange interaction between two identical metal ions through a cyano bridge.

Introduction

The cyanide ion has been known for a long time to be capable of bridging two transition metal atoms in an end−to−end fashion. Prussian blue, $[Fe_4\{Fe(CN)_6\}_3]\cdot xH_2O$, for instance, is considered to be the oldest known coordination compound[1] and has attracted during the last century the interest of many scientists trying to understand its puzzling structural[2−4] and physical properties, such as color,[5] magnetism,[6] and electrical conductivity.[5] Although it was soon obvious that the connection of iron atoms via cyano bridges is at the basis of all these phenomena, surprisingly, this finding did not trigger research attempts to synthesize model compounds in which the bonding and electronic structure could be analyzed in detail. In the past decades, the search for new molecule-based materials with tailored electric, optical, and/or magnetic properties has led to a renewed interest in Prussian blue analogues; this interest has been accompanied by a more systematic search and exploration of the physical properties of a number of attractive compounds based on the assembly of M−CN−M′ units.[7−9]

As far as the magnetic properties are concerned, the situation of cyano bridged polynuclear transition metal compounds is quite curious. The large amount of information that has been collected on hydroxo-, oxalato-, or azido-bridged dinuclear complexes of several transition metals has doubtlessly been decisive in the establishment of the emerging field of molecular magnetism. After the early years in which efforts were directed toward the simplest targets, i.e., dinuclear compounds with only one localized electron per metal center, a more or less clear picture of exchange coupling in these compounds has been established, and interest has shifted to the application of this knowledge to the synthesis of structures with higher dimensionality or of polynuclear clusters with complex magnetic

* To whom correspondence should be addressed.

(1) Anonymous, *Miscellanea Berolinensia ad incrementum scientiarum* (Berlin), **1710**, *1*, 377.
(2) Buser, H. J.; Ludi, A.; Petter, W.; Schwarzenbach, D. *J. Chem. Soc., Chem. Commun.* **1972**, 1299.
(3) Keggin, J. F.; Miles, F. D. *Nature* **1936**, *137*, 577.
(4) Ludi, A.; Güdel, H. U. *Struct. Bonding* **1973**, *14*, 1.
(5) Robin, M. R. *Inorg. Chem.* **1970**, *1*, 337.
(6) Ito, A.; Suenaga, M.; Ono, K. *J. Chem. Phys.* **1968**, *48*, 3597.
(7) Ferlay, S.; Mallah, T.; Ouahès, R.; Veillet, P.; Verdaguer M. *Nature* **1995**, *378*, 701.
(8) Holmes S. M.; Girolami, G. S. *J. Am. Chem. Soc.* **1999**, *121*, 5593.
(9) Hatlevik, O.; Buschmann, W. E.; Zhang, J.; Manson, J. L.; Miller, J. S. *Adv. Mater.* **1999**, *11*, 914.

10.1021/ic001420s CCC: $20.00
Published on Web 10/10/2001

behaviors. In the family of cyano-bridged compounds, however, the paucity of reports on dinuclear complexes is in sharp contrast with the large number of known structures in which cyanide ions link metal atoms to form one-, two-, and three-dimensional arrays, and the establishment of a fundamental understanding of bonding and exchange coupling in the simplest M−CN−M units has been skipped to move directly to the study of more complex structures.[10]

From the theoretical point of view, the cyano bridge possesses an interesting property that is lacking in the bridging units usually employed in molecular magnetism; it provides the most simple example of a disymmetric bridge in which both transition metals are in slightly different coordination surroundings. This lack of symmetry at the bridging ligand relating two metal centers may have important consequences for the exchange coupling. In particular, it is important to check if the localization of orbitals noticed in the heterobimetallic M−bridge−M′ units[11] is also observed when using the disymmetric cyano bridge in homometallic M−CN−M units. In this work, we report the results of a computational study of exchange coupling in homodinuclear cyano-bridged Cu(II) and Ni(II) complexes, which are the simplest models for understanding the relation between the magnetic behavior and the electronic structure in this family of compounds.

Experimental Section

WARNING! Although we have experienced no difficulties with the perchlorate salts and complexes described, these are potentially explosive and should be handled in small amounts, without heating, and with caution.

Tris(2-pyridylmethyl)amine (tmpa)[12] and $K_3[Cr(CN_6)]$[13] were synthesized using literature methods. All other reagents were purchased as reagent grade chemicals and used without further purification. All solvents were of analytical grade quality.

$[Cu_2(tren)_2CN](ClO_4)_3.H_2O$, A.[14] To a solution of copper perchlorate (1.53 g, 4 mmol) in water−acetonitrile (1:1, 20 mL) was added a solution of tris(aminoethyl)amine (0.58 g, 4 mmol, in water−acetonitrile, 1:1, 10 mL). The mixture was stirred for 20 min before adding potassium cyanide (0.130 g, 2 mmol) dissolved in a minimum amount of water. The solution was left standing for a few days, and the blue crystals that formed were collected and washed with ethanol. Yield 78%. Anal. Calcd for $C_{13}H_{38}Cu_2N_9Cl_3O_{13}$: C, 20.50; H, 4.99; N, 16.55; Cu, 16.69; Cl, 13.96. Found: C, 20.76; H, 4.85; N, 16.37; Cu, 16.52; Cl, 13.81. IR Spectrum (KBr, cm^{-1}) 2167 (CN). Electronic spectrum in CH_3CN: λ_{max}, nm (ϵ, l mol^{-1} cm^{-1}) 272 (9520), 780 (380). X-ray diffraction: chemical formula, $C_{13}H_{36}N_9Cu_2Cl_3O_{12}\cdot H_2O$; fw = 761.92; crystal system, tetragonal; space group = $P-4\ 2_1\ m$; $a = b =$ 11.580(1) Å, c = 11.299(3) Å, V = 1515.1(4) Å^3, Z = 2; R (R_w), 7.48% (9.58%).

$[Cu_2(tren)_2CN](BF_4)_3$, B. This complex was prepared following the procedure described for A $[Cu_2(tren)_2CN](ClO_4)_3\cdot H_2O$. Anal. Calcd for $C_{13}H_{36}Cu_2N_9B_3F_{12}$: C, 22.12; H, 5.14; N, 17.86. Found: C, 21.44; H, 5.14; N, 17.61. IR Spectrum (KBr, cm^{-1}) 2169 (CN). Electronic spectrum in CH_3CN: λ_{max}, nm (ϵ, l mol^{-1} cm^{-1}) 274 (12020), 785 (380). X-ray diffraction: chemical formula, $C_{13}H_{36}N_9Cu_2B_3F_{12}$; fw = 706; crystal system, tetragonal; space group = $P-4\ 2_1\ m$; $a = b =$ 11.492(2) Å, c = 11.019(2) Å, V = 1455.3(5) Å^3, Z = 2; R (R_w), 7.79% (8.86%).

$[Cu_2(tren)_2CN](PF_6)_2(ClO_4)\cdot 1/2\ KClO_4$, C. The complex was prepared by successively dissolving 0.740 g of $Cu(ClO_4)_2\cdot 6H_2O$, 0.3 mL of 2,2′,2″-tris(aminoethyl)amine (tren), 0.065 g of KCN, and 0.368 g of KPF_6 in 100 mL of warm distilled water. Dark blue crystals were obtained from the resulting solution by slow evaporation. Anal. Calcd for $C_{13}H_{36}Cl_{1.5}Cu_2K_{0.5}F_{12}N_9O_6P_2$: C, 17.27; H, 3.98; N, 13.94; F, 25.21; Cl, 5.88. Found: C, 17.32; H, 3.88; N, 13.75; F, 24.71; Cl, 5.58. X-ray diffraction: chemical formula, $C_{13}H_{36}N_9Cu_2Cl_{1.5}O_6K_{0.5}P_2F_{12}$; fw = 904.23; crystal system, tetragonal; space group = $I\bar{4}$; $a = b =$ 11.789(5) Å, c = 23.738(4) Å, V = 3299 (4) Å^3, Z = 4; R (R_w), 7.0% (7.7%).

$[Cu_2(tmpa)_2CN](ClO_4)_3$, D.[14] To a solution of tris(2-pyridylmethyl)-amine (0.25 g, 0.86 mmol) in water−acetonitrile (1:1, 20 mL) was added copper perchlorate (0.32 g, 0.86 mmol) dissolved in 10 mL of a similar mixture. The solution was stirred for 20 min before potassium cyanide (28 mg, 0.43 mmol) was added as a saturated aqueous solution. The solution was left standing for few days, and the turquoise−blue crystals that formed were collected and washed with ethanol. Yield 77%. Anal. Calcd for $[C_{37}H_{36}Cu_2N_9Cl_3O_{12}]$: C, 43.05; H, 3.52; N, 12.21. Found: C, 43.00; H, 3.39; N, 12.20. IR Spectrum (KBr, cm^{-1}) 2169 (CN). Electronic spectrum in CH_3CN: λ_{max}, nm (ϵ, l $mol^{-1}cm^{-1}$) 284 (7500), 823 (630). X-ray diffraction: chemical formula, $C_{37}H_{36}Cu_2N_9Cl_3O_{12}$; fw = 1032.19; crystal system, monoclinic; space group = $P2_1$; a = 12.494(6), b =9.689(2), c = 17.700(3) Å, β = 99.30(3)°, V = 2114(1) Å^3, Z = 2; R (R_w), 3.5% (4.1%).

$[Cu_2(tmpa)_2CN](BF_4)_3$, E. This complex was prepared following the procedure described for D $[Cu_2(tmpa)_2CN](ClO_4)_3$. Anal. Calcd for $[C_{37}H_{36}Cu_2N_9B_3F_{12}]$: C, 44.70; H, 3.65; N, 12.68. Found: C, 44.63; H, 3.76; N, 12.41. IR Spectrum (KBr, cm^{-1}) 2171 (CN). Electronic spectrum in CH_3CN: λ_{max}, nm (ϵ, l mol^{-1} cm^{-1}) 282 (6640), 833 (510). X-ray diffraction: chemical formula, $C_{37}H_{36}Cu_2N_9B_3F_{12}$; fw = 994.25; crystal system, monoclinic; space group = $P2_1$; a = 12.341(2), b =9.745(3), c = 17.456(2) Å, β = 99.41(1)°, V = 2070.9(8) Å^3, Z = 2; R (R_w), 5.64% (6.90%).

$[Cu_2(tmpa)_2CN](BF_4)_3\cdot(CH_3CN)_2$, F. This complex was prepared according to the procedure described for D using pure acetonitrile. After partial evaporation of the solvent, the solution was left standing for few days in a saturated ether atmosphere. The turquoise−blue crystals that had formed were collected and washed with ethanol. Yield 75%. Anal. Calcd for $C_{41}H_{42}Cu_2N_{11}B_3F_{12}$: C, 44.98; H; 3.72; N, 13.11. Found: C, 44.97; H, 3.90; N, 13.75. IR Spectrum (KBr, cm^{-1}) 2196 (CN). Electronic spectrum in CH_3CN: λ_{max}, nm (ϵ, l $mol^{-1}cm^{-1}$) 289 (5680), 835 (510). X-ray diffraction: cell parameters, crystal system, tetragonal; space group = $P4_32_12$; $a = b =$ 17.690(4) Å, c = 15.628(6) Å, V = 4891(2) Å^3, Z = 4; R (R_w), 7.5% (9.1%).

$[Ni_2(tetren)_2CN](ClO_4)_3$, G. To a solution of nickel perchlorate (1.462 g, 4 mmol) in water (10 mL) was added the tetraethylenepentamine (0.758 g, 4 mmol) dissolved in 10 mL of H_2O. The mixture was stirred for 20 min before adding potassium cyanide (0.130 g, 2 mmol) dissolved in a minimum amount of water. The solution was left standing for few days, resulting in the formation of pink crystals. Yield 68%. Anal. Calcd for $C_{17}H_{46}Ni_2N_{11}Cl_3O_{12}$: C, 24.35; H, 5.73; N, 18.38; Ni, 14.00; Cl, 12.68. Found: C, 24.63; H, 5.98; N, 18.16; Ni, 13.88; Cl, 12.95. IR spectrum (KBr, cm^{-1}) 2146 (CN). X-ray diffraction: cell parameters, crystal system, tetragonal; space group = $P4_2/ncm$; $a = b =$ 16.278(4) Å, c = 12.772(4) Å, V = 3384(2) Å^3; Z = 4; R (R_w), 8.5% (10.0%).

$[Ni_2(tetren)_2CN][Cr(CN)_6]\cdot 5H_2O$, H. To a solution of nickel perchlorate (2.187 g, 6 mmol) in water (20 mL) was added tetraethylenepentamine (1.154 g, 6.1 mmol) dissolved in 20 mL of H_2O. The solution was stirred for 20 min before adding potassium cyanide (0.194 g, 3 mmol) and $K_3[Cr(CN_6)]$ (0.325 g, 1 mmol) in a minimum amount of water. After an additional stirring of 20 min, the solution was left standing for few days, and the pink crystals that formed were collected. Anal. Calcd for $[C_{23}H_{56}CrNi_2N_{17}O_5]$: C, 33.68; H, 6.83; N, 29.03; Cr, 6.34; Ni, 14.31. Found: C, 33.97; H, 6.71; N, 28.79; Cr, 6.18; Ni, 14.22. IR spectrum (KBr, cm^{-1}) 2144 (CN bridge), 2127 (CN fixed on Cr). X-ray diffraction: chemical formula, $C_{43}H_{56}CrNi_2N_{15}O_5$; fw = 820.2; crystal system, monoclinic; space group = $P2_1/n$; a = 12.308 (3), b = 22.449(5), c = 13.779(2) Å, β = 96.75(1)°, V = 3781(6) Å^3, Z = 4; R (R_w), 5.79% (6.68%).

(10) Dunbar, K. M.; Heintz, R. A. *Prog. Inorg. Chem.* **1997**, *45*, 283.
(11) Cano, J.; Rodríguez-Fortea, A.; Alemany, P.; Alvarez, S.; Ruiz, E. *Chem. Eur. J.* **2000**, *6*, 327.
(12) Anderegg, G.; Wenk, F. *Helv. Chim. Acta* **1967**, *50*, 2330.
(13) Ferlay, S.; Mallah, T.; Ouahes, R.; Veillet, P.; Verdaguer M. *Inorg. Chem.* **1999**, *38*, 229.
(14) The present paper was ready for submission when the following paper reporting similar Cu(II) complexes appeared: Parker, R. J.; Spiccia, L.; Moubaraki, B.; Murray, K. S.; Skelton, B. W.; White, A. H. *Inorg. Chim. Acta* **2000**, *30*, 922.

Table 1. Crystallographic Data for $[Cu_2(tren)_2CN](ClO_4)_3 \cdot H_2O$, $[Cu_2(tren)_2CN](ClO_4)(PF_6)_2 \cdot 1/2KClO_4$, $[Cu_2(tmpa)_2CN](ClO_4)_3$, and for the nickel complex $[Ni_2(tetren)_2CN][Cr(CN_6)] \cdot 5H_2O$.

	$[Cu_2(tren)_2CN](ClO_4)_3 \cdot H_2O$	$[Cu_2(tren)_2CN](ClO_4)(PF_6)_2 \cdot 1/2KClO_4$	$[Cu_2(tmpa)_2CN](ClO_4)_3$	$[Ni_2(tetren)_2CN][Cr(CN)_6] \cdot 5H_2O$
chem formula	$C_{13}H_{38}N_9Cu_2Cl_3O_{13}$	$C_{13}H_{36}N_9Cu_2Cl_{1.5}O_6,K_{0.5}P_2F_{12}$	$C_{37}H_{36}N_9Cu_2Cl_3O_{12}$	$C_{23}H_{56}CrNi_2N_{17}O_5$
fw	761.94	904.23	1032.19	820.2
cryst syst	tetragonal	tetragonal	monoclinic	monoclinic
a (Å)	11.580(1)	11.789(5)	12.494(6)	12.308(3)
b (Å)	11.580(1)	11.789(5)	9.689(2)	22.449(5)
c (Å)	11.299(3)	23.738(4)	17.700(3)	13.778(2)
α (deg)	90	90	90	90
β (deg)	90	90	99.30(3)	96.75(1)
γ (deg)	90	90	90	90
V (Å^3)	1515.1(4)	3299 (4)	2114(1)	3781(6)
Z	2	4	2	4
space group	$P\bar{4}2_1m$	$I\bar{4}$	$P2_1$	$P2_1/n$
cryst shape	parallelepiped	parallelepiped	needles	needles
cryst color	blue	blue	turquoise−blue	pink
nb of data collected	2517	2043	4150	3873
Nb of unique data collected	1328		3952	3523
nb of data used for refinement	812 $(F_o)^2 > 3\sigma(F_o)^2$	1545 $(F_o)^2 > 3\sigma(F_o)^2$	3136 $(F_o)^2 > 3\sigma(F_o)^2$	1216 $(F_o)^2 > 3\sigma(F_o)^2$
R^a	0.0748	0.070	0.0346	0.0579
$R_w{}^a$	0.0958	0.077	0.0408	0.0668
nb of variables	106	236	560	190
$\Delta\rho$min (e/Å^3)	−0.43	−0.49	−0.39	−0.34
$\Delta\rho$max (e/Å^3)	0.70	1.04	0.40	0.58

[a] $R = \sum||F_o| - |F_c||/\sum|F_o|$, $R_w = [\sum w(|F_o| - |F_c|)^2/\sum wF_o^2]^{1/2}$.

X-ray Crystallography. Crystals suitable for X-ray crystallography were directly obtained from the reaction medium or by recrystallization from water/acetonitrile solutions. For all the structures herein described, accurate cell dimensions and orientation matrixes were obtained by least-squares refinements of 25 accurately centered reflections on a Enraf Nonius CAD4 diffractometer equipped with graphite-monochromatic Mo Kα radiation. No significant variations were observed in the intensities of two checked reflections during data collections. Absorption corrections were applied using Ψ scan method. Computation was performed by using the PC version of Crystals.[15] Scattering factors and corrections for anomalous dispersion were taken from Cromer.[16] The structures were solved with SHELX86[17] followed by Fourier maps technique and refined by full-matrix least squares with anisotropic thermal parameters for all non-hydrogen atoms, when sufficient data were available. Crystallographic data and details of the refinements are reported as Supporting Information and in a condensed form in Table 1.

Physical Characterization. Electronic spectra were obtained with a UV 210 PC Shimadzu spectrophotometer. IR spectra were recorded between 4000 and 250 cm^{-1} on a Bio-Rad FTS 165 FT-IR spectrometer on KBr pellets. DC magnetic susceptibility measurements were carried out on a Quantum Design MPMS SQUID susceptometer equipped with a 5 T magnet and operating in the temperature range from 1.8 to 400 K.

Computational Methodology. Since detailed descriptions of the computational strategy adopted in this work can be found elsewhere,[18−25] we will outline here only its most relevant aspects. Using a phenomenological Heisenberg Hamiltonian $\hat{H} = -J\hat{S}_1\hat{S}_2$ to describe the exchange coupling in a dinuclear compound, the coupling constant *J* can be related to the energy difference between the lowest and highest spin states. For the case in which $S_1 = S_2$, the coupling constant may be obtained by using the following equation

$$E_{HS} - E_{LS} = -2JS_i(S_i + 1/2) \quad (1)$$

where E_{HS} is the energy that corresponds to the state with the highest total spin, E_{LS} corresponds to the state with the lowest total spin ($S = 0$, for a homodinuclear complex), and S_i is the total spin on each metal atom.

In recent work we have shown that, when using DFT-based wave functions, a reasonable estimate of the energy corresponding to the low spin state, E_{LS}, can be obtained directly from the energy of a broken-symmetry solution E_{BS}. In this case, introducing $S_i = 1/2$ or 1 for the copper and nickel dinuclear compounds, respectively, we arrive to the following expressions for *J*:

$$J_{Cu-Cu} = E_{BS} - E_{HS} \quad (2)$$

$$3J_{Ni-Ni} = E_{BS} - E_{HS} \quad (3)$$

Experience has shown that these equations, in which the energy of the low spin state is estimated directly from the energy of the broken-symmetry solution without performing any spin projection, leads to excellent agreement with experimental data for a large variety of compounds with exchange coupled electrons. For a more thorough discussion the reader is referred to previous work.[18−25]

At a practical level, the evaluation of the coupling constant of each compound requires two separate calculations, one for the high spin state and another one for the low spin, broken symmetry state. The

(15) Crystals: Watkin, D. J.; Carruthers, J. R.; Betteridge, P. W. Chemical Crystallography Laboratory; University of Oxford, Oxford, UK, 1988.
(16) Cromer, D. T. *International Tables for X-ray Crystallography*; Kynoch: Birmingham, UK, **1974**; Vol IV.
(17) Sheldrick, G. M. *SHELXS 86: "A program for Crystal Structure Determination"*; University of Göettingen: Germany, 1986.
(18) Ruiz, E.; Alemany, P.; Alvarez, S.; Cano, J. *Inorg. Chem.* **1997**, *36*, 3683.
(19) Ruiz, E.; Alemany, P.; Alvarez, S.; Cano, J. *J. Am. Chem. Soc.* **1997**, *119*, 1297.
(20) Ruiz, E.; Cano, J.; Alvarez, S.; Alemany, P. *J. Am. Chem. Soc.* **1998**, *120*, 11122.
(21) Ruiz, E.; Alvarez, S.; Alemany, P. *Chem. Commun.* **1998**, 2767.
(22) Ruiz, E.; Cano, J.; Alvarez, S.; Alemany, P. *J. Comput. Chem.* **1999**, *20*, 1391.
(23) Cano, J.; Alemany, P.; Alvarez, S.; Verdaguer, M.; Ruiz, E. *Chem. Eur. J.* **1998**, *4*, 476.
(24) Cano, J.; Ruiz, E.; Alemany, P.; Lloret, F.; Alvarez, S. *J. Chem. Soc., Dalton Trans.* **1999**, 1669.
(25) Fabrizi di Biani, F.; Ruiz, E.; Cano, J.; Novoa, J. J.; Alvarez, S. *Inorg. Chem.* **2000**, *39*, 3221.

hybrid, DFT-based B3LYP method[26] has been used in all calculations as implemented in Gaussian-94,[27] mixing the exact Hartree−Fock exchange with Becke's expression for the exchange functional,[28] and using the Lee−Yang−Parr correlation functional.[29] The double-ζ quality basis set proposed by Ahlrichs et al.[30] has been employed for all atoms except for the metal ones, for which the triple-ζ basis set[31] proposed by the same authors is used.

The experimental magnetic susceptibility is measured from solid samples in which packing forces can induce small deviations from the minimum energy structure of the individual molecules. To be able to compare our computed coupling constants for complete structures with the experimental values, we used in our calculations the molecular structure as determined experimentally rather than an optimized one, in which small changes with respect to the experimental structure could result in significant deviations for the coupling constant.

Results and Discussion

Syntheses and Characterization. New copper and nickel homodinuclear complexes, based on tetra- and pentadentate polyamine ligands and linked by a cyano bridge, were synthesized[14] in order to better correlate structural and magnetic properties. Concerning the copper complexes, two different coordination modes of the transition metal cations appeared and will be discussed together with the influence of the polyamine ligand itself. To prevent the oxidation of cyanide to cyanogen from Cu(II),[32] tris(2-aminoethyl)amine (tren) and tris(2-pyridylmethyl)amine (tmpa)[12] have been used as tetradentate ligands since they are expected to give stable complexes with a trigonal bipyramidal geometry. In the present paper, the related complexes, $[Cu_2(tren)_2CN](ClO_4)_3 \cdot H_2O$, **A**, and $[Cu_2(tmpa)_2CN](ClO_4)_3$, **D**, are compared to $[Cu_2([14]\text{-}4\text{-}11\text{-}dieneN_4)_2CN](ClO_4)_3$, which has been already published in the literature[33] and viewed as a model compound for another coordination mode close to the square pyramidal geometry. For the purpose of analogy between the different products, perchlorate salts have been used in the synthesis, but similar compounds with equivalent properties have been obtained with tetrafluoroborate anions. Regarding the nickel complexes, a commercially available tetraethylenepentamine (tetren) ligand has been used for the synthesis of two binuclear nickel complexes, $[Ni_2(tetren)_2CN](ClO_4)_3$ and $[Ni_2(tetren)_2CN][Cr(CN_6)] \cdot 5H_2O$. The ligands used in these studies are depicted in **1**.

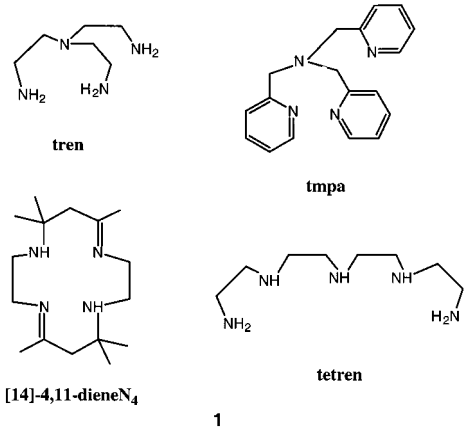

1

Some of the described compounds were first obtained as byproducts from the hydrolytic decomposition of inorganic precursors such as $K_3[Cr(CN_6)]$. Nevertheless, these dinuclear compounds were also successfully synthesized using mononuclear copper or nickel complexes and potassium cyanide in stoichiometric proportions. The point is the use of mononuclear species as building blocks, such as $[CuL(H_2O)]^{2+}$ and $[NiL(H_2O)]^{2+}$ complexes, in which L is a multidentate ligand blocking all the coordination sites except one occupied by a labile solvent molecule that can be easily replaced by the cyano group. All the dinuclear complexes have been isolated as single crystals and fully characterized. The elemental analysis and electronic spectra are in good agreement with the expected structures. In all cases, the infrared spectra show a unique band in the range of 2145−2169 cm^{-1}, characteristic of the asymmetric stretching vibration of a bridging cyanide for copper and nickel complexes. Specific attention must be paid to the dinuclear nickel compound in which the $[Cr(CN_6)]^{3-}$ anion plays the role of the counterion. In such a case, two bands are detected in the 2100−2200 cm^{-1} range, one at 2127 cm^{-1}, corresponding to the cyanide of the hexacyanochromate(III), and the other at a higher energy, 2145 cm^{-1}, which is attributed to the cyano bridge between the two nickel metal ions.

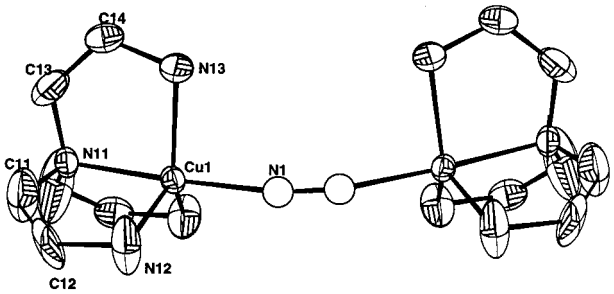

Figure 1. Structure of the cation in $[Cu_2(tren)_2CN](ClO_4)_3 \cdot H_2O$.

Structural Studies. Regarding the copper compounds, two series of complexes derived from tren and tmpa were prepared and provide comparative structural data. The structures, differing from one another by the nature of the ligand, of the counteranion or the cocrystallized salt or solvent are the following, $[Cu_2(tren)_2CN](ClO_4)_3 \cdot H_2O$,[14] **A**, and $[Cu_2(tren)_2CN](BF_4)_3$, **B** (isostructural); $[Cu_2(tren)_2CN](PF_6)_2(ClO_4)$ with a cocrystallized 1/2 $KClO_4$, **C**; $[Cu_2(tmpa)_2CN](ClO_4)_3$,[14] **D**, $[Cu_2(tmpa)_2CN](BF_4)_3$ (isostructural), **E**; and $[Cu_2(tmpa)_2CN](ClO_4)_3(CH_3CN)_2$, **F**. The $[Cu_2([14]\text{-}4\text{-}11\text{-}dieneN_4)_2CN](ClO_4)_3$ complex is known from a previous work.[33] Because of the large amount of structural information presented here and the similarities that will be first discussed, some results might be expressed as ranges of values rather than individual ones, and only two structures (**A** and **D**) will be fully described. The perspective views of the reference structures are set out in Figures 1 and 2, and selected metric data are compiled in Table 2.

Despite the variety of the crystal structures, the data describing the molecular entities $[Cu_2(tmpa)_2CN]^{3+}$ indicate a remarkable similarity. For instance, the C−N bond lengths and both

(26) Becke, A. D. *J. Chem. Phys.* **1993**, *98*, 5648.
(27) Frisch, M. J.; Trucks, G. W.; Schlegel, H. B.; Gill, P. M. W.; Johnson, B. G.; Robb, M. A.; Cheeseman, J. R.; Keith, T. A.; Petersson, G. A.; Montgomery, J. A.; Raghavachari, K.; Al-Laham, M. A.; Zakrzewski, V. G.; Ortiz, J. V.; Foresman, J. B.; Ciolowski, J.; Stefanov, B. B.; Nanayakkara, A.; Challacombe, M.; Peng, C. Y.; Ayala, P. Y.; Chen, W.; Wong, M. W.; Andres, J. L.; Replogle, E. S.; Gomperts, R.; Martin, R. L.; Fox, D. J.; Binkley, J. S.; Defrees, D. J.; Baker, J.; Stewart, J. J. P.; Head-Gordon, M.; Gonzalez, M.; Pople, J. A. *Gaussian94*; Gaussian, Inc.: Pittsburgh, PA, 1994.
(28) Becke, A. D. *Phys. Rev. A* **1988**, *38*, 3098.
(29) Lee, C.; Yang, W.; Parr, R. G. *Phys. Rev. B* **1988**, *37*, 785.
(30) Schaefer, A.; Horn, H.; Ahlrichs, R. *J. Chem. Phys.* **1992**, *97*, 2571.
(31) Schaefer, A.; Huber, C.; Ahlrichs, R. *J. Chem. Phys.* **1994**, *100*, 5829.
(32) Scott, M. J.; Lee, S. C.; Holm, R. H. *Inorg. Chem.* **1994**, *33*, 4651, and references therein.
(33) Jungst, R.; Stucky, G. *Inorg. Chem.* **1974**, *13*, 2404.

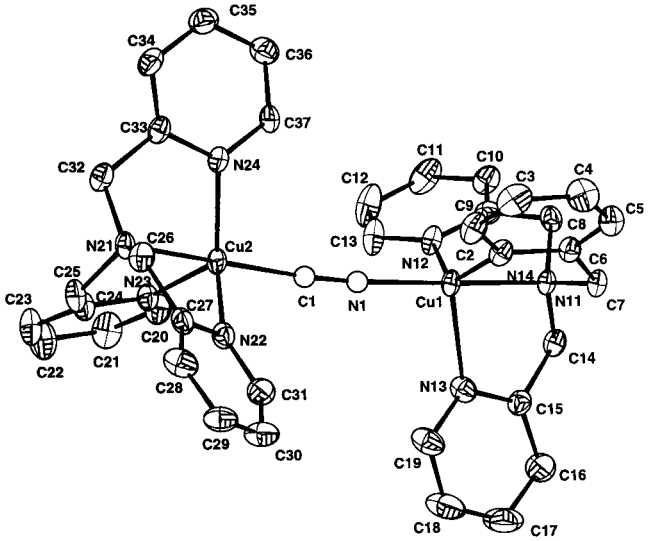

Figure 2. Structure of the cation in $[Cu_2(tmpa)_2CN](ClO_4)_3$.

Table 2. Selected Bond Lengths and Angles in $[Cu_2(tren)_2CN](ClO_4)_3 \cdot H_2O$, $[Cu_2(tmpa)_2CN](ClO_4)_3$, and $[Cu_2([14]\text{-}4\text{-}11\text{-}dieneN_4)_2CN](ClO_4)_3$

	$[Cu_2(tren)_2CN](ClO_4)_3 \cdot H_2O$	$[Cu_2(tmpa)_2CN](ClO_4)_3$ Cu(1)	$[Cu_2(tmpa)_2CN](ClO_4)_3$ Cu(2)	$[Cu_2([14]\text{-}4\text{-}11\text{-}dieneN_4)_2CN](ClO_4)_3$[a]
Interatomic Distances (Å)				
C−N bridge[b]	1.13 (3)	1.151 (7)		1.147 (6)
Cu−cyanide[b]	1.98 (2)	1.982 (6)	1.966 (6)	2.125 (3)
Cu−N(11)	2.02 (1)	2.026 (5)	2.047 (5)	2.057 (4)
Cu−N(12)	2.06 (2)	2.044 (5)	2.061 (5)	2.035 (4)
Cu−N(13)	2.07 (1)	2.137 (5)	2.131 (5)	2.056 (4)
Cu−N(14)	*c*	2.029 (5)	2.024 (5)	2.018 (4)
Bond Angles (°)				
Cu−C(1)−N(1) cyanide	165.7 (4)	174.9 (5)	175.5 (5)	178.6 (5)
N(11)−Cu−cyanide	175.6 (6)	178.8 (2)	179.5 (3)	93.3 (1)
N(12)−Cu−cyanide	101.1 (7)	99.2 (2)	98.9 (2)	113.7 (2)
N(13)−Cu−cyanide	93.2 (4)	100.1 (2)	101.0 (2)	92.7 (1)
N(14)−Cu−cyanide	*c*	97.9 (2)	98.2 (2)	111.7 (2)
N(11)−Cu−N(12)	83.3 (7)	79.9 (2)	80.9 (2)	93.6 (2)
N(11)−Cu−N(13)	84.4 (4)	80.9 (2)	79.5 (2)	174.0 (1)
N(11)−Cu−N(14)	*c*	82.3 (2)	81.7 (2)	84.4 (2)
N(12)−Cu−N(13)	121.0 (5)	106.8 (2)	106.8 (2)	83.1 (1)
N(12)−Cu−N(14)	*c*	134.4 (2)	134.6 (2)	134.6 (1)
N(13)−Cu−N(14)	114.7 (11)[d]	111.3 (2)	110.7 (2)	94.2 (2)

[a] See ref 33. [b] Since the cyanide is disordered, only an average distance is given. [c] N(13) and N(14) are equivalent by symmetry. [d] Atoms in position $1/2 + y, -1/2 + x, z$.

the Cu−C−N and N−C−Cu angles of the cyano bridge are almost identical (1.15 Å and 175°, respectively), and the dihedral angle reflects a cisoid conformation (19°). Aside from the perchlorate and tetrafluoroborate isostructural complexes, similarities are also observed for the **D**, **E**, and **F** species, despite their different packing modes. To a lesser extent, due to the strong bending of the cyano bridge (165°), this trend is also valid for the $[Cu_2(tren)_2CN]^{3+}$ compounds.

The $[Cu_2(tren)_2CN]^{3+}$ complex, when crystallized as a perchlorate, **A**, or a tetrafluoroborate salt, **B**, occurs as a symmetric cation with undistinguishable bridge atoms. Concerning the structures **D** and **E**, in which there is no inversion center, the Cu bridge bond length or anisotropic thermal parameters do not allow for distinction between the carbon and the nitrogen atoms.

Despite the disorder observed in all structures for the CN bridges, the X-ray diffraction data allow us to determine the coordination mode around the transition metal and the geometrical deformation of the cyanide bridging ligand. The two metallic atoms are equivalent with an identical environment. As expected, in the complexes $[Cu_2(tren)_2CN](ClO_4)_3 \cdot H_2O$, **A**, $[Cu_2(tmpa)_2CN](ClO_4)_3$, **D**, and their analogues, bond angles and distances (Table 2) are consistent with a trigonal bipyramid structure having the cyanide in an axial position. In contrast, in $[Cu_2([14]\text{-}4\text{-}11\text{-}dieneN_4)_2CN](ClO_4)_3$, the geometry about the transition metal atom is a distorted trigonal bipyramid in which the cyanide ion is bridging from an equatorial position, as previously described.[33]

Table 3. Selected Bond Lengths and Angles in $[Ni_2(tetren)_2CN][Cr(CN_6)] \cdot 5H_2O$

	Ni (1)	Ni (2)
Interatomic Distances (Å)		
C−N bridge[b]	1.16 (2)	
Ni−cyanide[b]	2.04 (2)	2.04 (2)
Ni−N(11)	2.11 (2)	2.14 (1)
Ni−N(12)	2.10 (1)	2.11 (2)
Ni−N(13)	2.12 (2)	2.16 (2)
Ni−N(14)	2.13 (2)	2.16 (1)
Ni−N(15)	2.15 (2)	2.11 (2)
Bond Angles (°)		
Ni−C(1)−N(1) cyanide	173.6 (3)	174.2 (3)
N(11)−Ni−cyanide	90.0 (6)	92.8 (5)
N(12)−Ni−cyanide	92.7 (6)	95.7 (5)
N(13)−Ni−cyanide	172.9 (6)	91.2 (6)
N(14)−Ni−cyanide	92.0 (6)	168.3 (5)
N(15)−Ni−cyanide	90.7 (5)	88.4 (5)
N(11)−Ni−N(12)	82.2 (6)	80.7 (6)
N(11)−Ni−N(13)	94.6 (6)	163.7 (6)
N(11)−Ni−N(14)	176.5 (6)	94.5 (6)
N(11)−Ni−N(15)	94.3 (6)	94.0 (6)
N(12)−Ni−N(13)	82.7 (6)	83.1 (6)
N(12)−Ni−N(14)	100.6 (6)	94.5 (6)
N(12)−Ni−N(15)	175.1 (6)	173.4 (6)
N(13)−Ni−N(14)	83.6 (7)	84.4 (6)
N(13)−Ni−N(15)	94.2 (6)	102.0 (6)
N(14)−Ni−N(15)	82.8 (3)	82.0 (6)

[a] For Ni(2), only the last figure of the nitrogen numbers have to be considered. [b] Since the cyanide is disordered, only an average distance is given.

Regarding the two nickel compounds, two structures have been resolved, $[Ni_2(tetren)_2CN][Cr(CN_6)] \cdot 5H_2O$ and $[Ni_2(tetren)_2CN](ClO_4)_3$, although only partial information have been obtained for the latter. The quality of the crystals being good enough, this is probably due to the disorder induced by the different conformations of the flexible ligand. It is well known[34] that such pentadentate linear ligands may adopt more than eight different conformers around a transition metal in an octahedral geometry. The best evidence of such situation may be the structure of $[Ni_2(tetren)_2CN][Cr(CN_6)] \cdot 5H_2O$ itself, in which the two nickel atoms are not equivalent and behave as two different conformers. To better appreciate this effect, one has to consider the central amine position of the ligand. Despite this distinction between the two nickel atoms, the uncertainty in the orientation of the CN bridge remains. Significant crystallographic data concerning $[Ni_2(tetren)_2CN][Cr(CN_6)] \cdot 5H_2O$ are reported in Table 3.

Magnetic Properties. For the $[Cu_2(tren)_2CN]^{3+}$ perchlorate **A**, the $\chi_M T$ product (χ_M is the magnetic susceptibilty per two copper(II) ions) decreases continuously when cooling from room temperature to 2.0 K (Figure 3a). The value of $\chi_M T$ at 300 K is 0.65 $cm^3\ mol^{-1}$ K (significantly smaller than that expected for two magnetically isolated spin doublets: 0.827 $cm^3\ mol^{-1}$ K with $g = 2.10$), and $\chi_M T$ becomes practically zero at temperatures below 50 K. The susceptibility curve exhibits a maximum at ca. 165 K. All these features are consistent with the occurrence of a strong antiferromagnetic coupling between two copper(II)

(34) House, D. A. *Coord. Chem. Rev.* **1977**, 257.

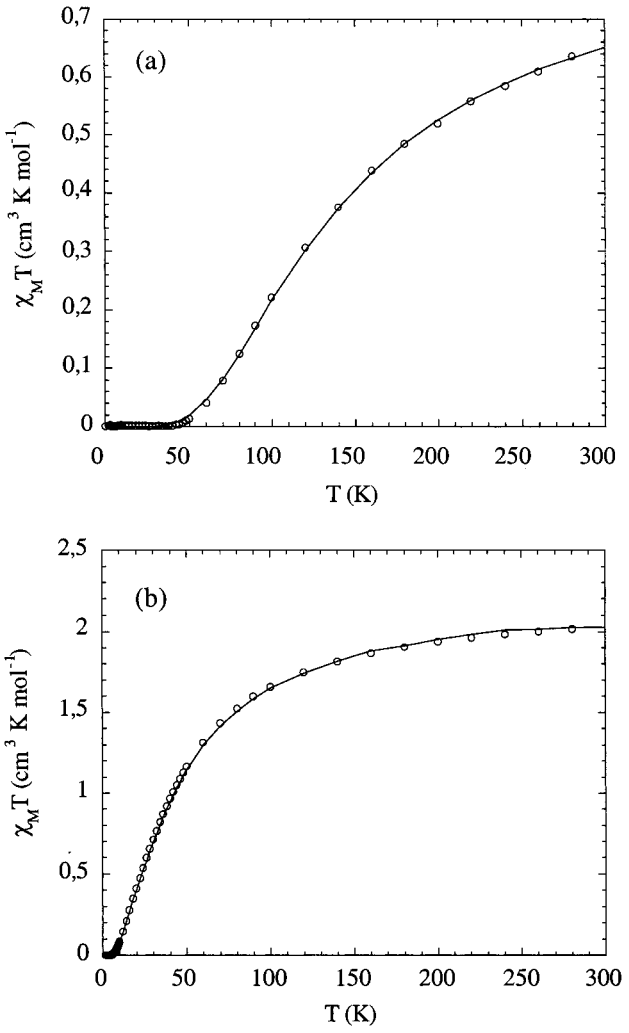

Figure 3. (a) Thermal dependence of the molar susceptibility of $[Cu_2(tren)_2CN](ClO_4)_3 \cdot H_2O$ (○ experiment; — best fit). (b) Thermal dependence of the molar susceptibility of $[Ni_2(tetren)_2CN](ClO_4)_3$ (○ experiment; — best fit).

ions (two local spin doublets), the low-lying spin state being a singlet. Least-squares fitting of the susceptibility data through a simple Bleaney−Bowers expression derived through the Hamiltonian $\hat{H} = -J\hat{S}_1\hat{S}_2$ ($S_1 = S_2 = 1/2$) leads to $J = -157$ cm^{-1}, $g = 2.15$, and $R = 1.08 \times 10^{-4}$. R is the agreement factor defined as $\sum i[(\chi_M)_{obs}(i) - (\chi_M)_{calc}(i)]^2/\sum i[(\chi_M)_{obs}(i)]^2$. The theoretical curve matches the magnetic data in the whole temperature range very well, as indicated by the low value of R.

Magnetic measurements were performed on each of the dinuclear complexes, and similar results were obtained for equivalent compounds (Table 4, see also ref 14). As expected, the thermal dependence of the molar susceptibility, measured on a SQUID magnetometer, indicates that $\chi_M T$ decreases upon cooling from 300 to 2 K (Figure 3). These results demonstrate the short-range antiferromagnetic exchange interaction between the two identical atoms. Consequently, in all cases the susceptibility becomes zero at low temperature, except for $[Ni_2(tetren)_2CN][Cr(CN_6)] \cdot 5H_2O$ in which the chromicyanide behaves as a paramagnetic species. The $\chi_M T$ value measured for this compound at 2 K is 1.85 cm^3 K mol^{-1}, which is in good agreement with the theoretical estimate based on the Curie law for an isolated chromium(III) atom.

More interesting is the evaluation of the exchange coupling constant for the various complexes. The experimental $\chi_M T = f(T)$ data were fitted to the simple analytical expressions obtained from the Hamiltonian with isotropic interaction between the two metallic ions:

$$\chi_M T = \frac{2N(g\beta)^2}{k}\left[\frac{\exp(-J/kT)}{1 + 3\exp(-J/kT)}\right] \quad (4)$$

$$\chi_M T = \frac{2N(g\beta)^2}{k}\left[\frac{\exp(-J/kT) + 5\exp(-3J/kT)}{1 + 3\exp(-J/kT) + 5\exp(-3J/kT)}\right] \quad (5)$$

for copper and nickel complexes, respectively.

Concerning the copper compounds, the resulting J values are -157 and -100 cm^{-1} for $[Cu_2(tren)_2CN]^{3+}$ and $[Cu_2(tmpa)_2CN]^{3+}$, respectively, with an agreement factor close to 1. The difference between the two families of compounds will be discussed in the following part of this paper.

Regarding the dinuclear nickel complexes, very similar J values were obtained, -24.5 cm^{-1} ($g = 2.09$) for $[Ni_2(tetren)_2CN](ClO_4)_3$ and -24.8 cm^{-1} ($g = 2.10$) for $[Ni_2(tetren)_2CN][Cr(CN_6)] \cdot 5H_2O$. All of our attempts to get other complexes with diversified geometries and different J values were unsuccessful.

Theoretical Studies for Dinuclear Cu(II) Compounds. We begin with the simplest case of a cyanide-mediated exchange coupled system involving transition metals, i.e., a complex with two cyano-bridged Cu(II) ions where the cyanide ion is coordinated to the metal atoms in an end−to−end fashion. The local copper atom environments in the dinuclear compounds of this type are distorted trigonal bipyramids. The exchange interaction between the unpaired electrons is always antiferromagnetic, with coupling constants covering a wide range (-183 to -9 cm^{-1}). Two distinct situations can be recognized from the available structural and magnetic information.[35] When the cyanide ion is bridging two equatorial sites (**2**), the coupling is weakly antiferromagnetic, with coupling constants on the order of -10 cm^{-1}.

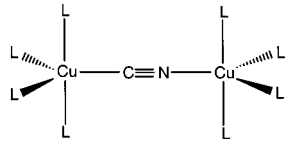

2

On the other side, when the cyanide ion is bridging two axial sites (**3**), the coupling is strongly antiferromagnetic, with coupling constants of up to -183 cm^{-1}.

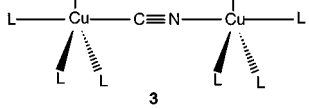

3

The situation is, however, complicated in the experimentally determined structures by distortions in both the coordination environment around the copper atoms and the relative disposition of the cyanide ion with respect to the Cu−Cu axis.[33]

In a first attempt to theoretically investigate the exchange coupling in this family of compounds, we focus on the idealized model structures depicted in **2** and **3**, in which each copper atom is surrounded by four ammonia molecules with the cyanide ion in the fifth coordination position. The angles formed by the ligands and the copper atom correspond to those of a perfect trigonal bipyramid, i.e., $L_{eq}-Cu-L_{eq} = 120°$, $L_{eq}-Cu-L_{ax} =$

(35) Bieksza, D. S.; Hendrickson, D. N. *Inorg. Chem.* **1977**, *16*, 924.

Table 4. IR Data, M−C−N Angles, Best Fitted Coupling Constants, g Values, and Calculated J Values of All the Complexes

	ν_{CN} (cm^{-1})	M−C−N (°)	$J_{exp.}$ (cm^{-1})	g	$J_{calc.}$ (cm^{-1})
$[Cu_2(tren)_2CN](ClO_4)_3 \cdot H_2O$	2167	165.7	−157.5	2.15	
$[Cu_2(tren)_2CN](BF_4)_3$	2169	167.3	−160.0	2.13	
$[Cu_2(tren)_2CN](ClO_4)(PF_6)_2 \cdot 1/2KClO_4$	2169	162.0	−183	2.12	−109
$[Cu_2(tmpa)_2CN](ClO_4)_3$	2169	174.9−175.5	−103.9	2.10	−54
$[Cu_2(tmpa)_2CN](BF_4)_3$	2171	174.0	−100.0	2.13	
$[Cu_2(tmpa)_2CN](BF_4)_3 \cdot (CH_3CN)_2$	2196	174.5	−98.6	2.13	
$[Ni_2(tetren)_2CN][Cr(CN)_6] \cdot 5H_2O$	2144	173.6−174.2	−24.5	2.09	−20.5
$[Ni_2(tetren)_2CN](ClO_4)_3$	2146	171.5	−24.8	2.10	−19.8

90°, and $L_{ax}-Cu-L_{ax} = 180°$. The $Cu-N_{term}$ distance has been taken as 2.05 Å, the average value found in the experimentally determined structures. For the ammonia molecules, the geometrical parameters that were used are $H-N_{term} = 1.015$ Å and $H-N_{term}-Cu = 109°$. The experimental determination of the bridge geometry is prevented by the disorder between the C and N atoms, and an average distance of 2.00 Å was taken for both the Cu−C and Cu−N bonds. The C−N bond length adopted in all model structures was 1.14 Å.

The evaluation of the coupling constant for model structures **2** and **3** yields values of −18.6 and −103 cm^{-1}, respectively. The trend is in agreement with that found for the experimental data; when the cyano bridge is between two axial positions of the copper coordination sphere, the antiferromagnetic coupling is significantly stronger. This behavior can be easily rationalized using qualitative MO arguments. According to the model proposed by Hay, Thibeault, and Hoffmann (HTH model)[36] for the exchange interaction between two electrons located on two weakly interacting centers, the antiferromagnetic contribution to the coupling constant is proportional to the square of the energy gap separating both singly occupied molecular orbitals (SOMOs) in the triplet state. For a trigonal bipyramidal coordination environment, the two SOMOs are mainly formed by the d_{z^2}-type orbitals of the copper atoms (z being the direction of the trigonal axis), with some admixture of CN-centered orbitals. As noted by Bieksza and Hendrickson,[35] the two trigonal bipyramids in **3** are oriented in such a way that the main lobes of the copper d_{z^2}-type orbitals are pointing toward the bridging cyanide ion. The large overlap between these orbitals results in a relatively large gap between the two SOMOs (**4a**), thus favoring the antiferromagnetic interaction.

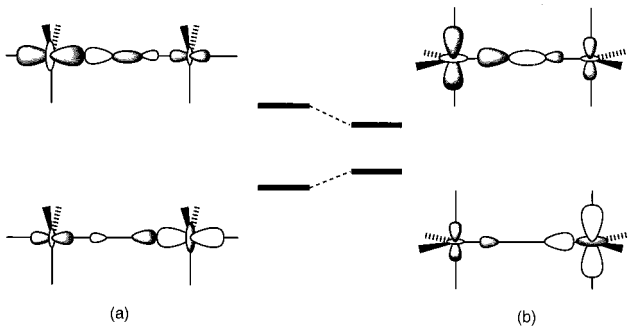

4

For model structure **2**, the molecular orbitals of the cyanide ion can only interact with the torus of the metal-centered d_{z^2}-type orbitals, and the weaker overlap leads to a smaller energy gap between the SOMOs and, hence, to a weaker antiferromagnetic coupling (**4b**). The analysis of the Kohn−Sham SOMOs for the triplet states of the two models supports this explanation.

(36) Hay, P. J.; Thibeault, J. C.; Hoffmann, R. *J. Am. Chem. Soc.* **1975**, *97*, 4884.

As mentioned earlier, the experimentally determined structures differ, sometimes significantly, from the idealized models used above. In this respect, it is interesting to analyze the effect of the most important structural distortions on the exchange coupling, hoping that the understanding of these effects will help to design new compounds with fine-tuned magnetic properties. The first distortion analyzed consists of bending the ligands in the idealized structure **2** until a square pyramidal coordination environment on both copper atoms is reached (achieved by simultaneously increasing α and decreasing β, as shown in **5**).

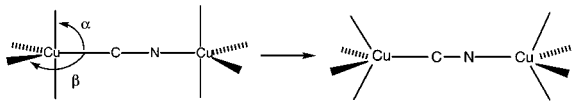

5

This motion of the terminal ligands reduces the magnitude of the coupling constant from −18.6 cm^{-1} in model **2** to only −1.0 cm^{-1} for a square pyramidal coordination, with $\alpha = \beta = 110°$ on both Cu atoms. Changing the value of these angles while maintaining the square pyramidal coordination around the copper atoms results in a negligible change in the exchange coupling constant, which remains around −1.0 cm^{-1}.

The almost negligible coupling found in the model with square pyramidal coordination around the copper atoms can be easily rationalized using the same MO-based arguments as above. When distorting the trigonal bypiramidal environment to that of a square pyramid, the d orbital on the copper atom bearing the unpaired electron changes its character gradually from d_{z^2}-type to $d_{x^2-y^2}$-type. The δ type symmetry of the $d_{x^2-y^2}$ orbitals with respect to the Cu−Cu axis (**6**) prevents interaction with the orbitals of the cyano bridge, and the energy gap between the two SOMOs becomes very small.

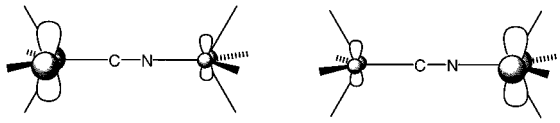

6

As a result, according to the HTH model, the antiferromagnetic contribution to J becomes negligible.

An analysis of the relative energy of the singlet states of the distorted molecules shows that the trigonal-bipyramidal coordination sphere is the most stable one. The structure with the copper atoms in a square pyramidal coordination with $\alpha = \beta = 110°$ is about 20 kJ/mol higher in energy, but square pyramids with different angles ($\alpha = \beta$) are further destabilized (e.g., 100 kJ/mol for $\alpha = \beta = 90°$, or 400 kJ/mol for $\alpha = \beta = 120°$).

A possible distortion in compounds with a structure of type **2** is the displacement of the cyanide ion away from the Cu−Cu vector. Two different possibilities for this movement could be envisaged, the cisoid and the transoid distortions shown in **7**. The effect of these distortions on the coupling constant (Figure

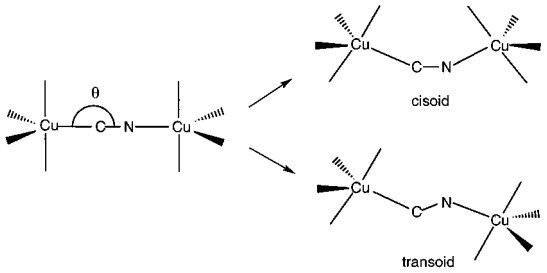

7

4a) for reasonable deviations of the cyanide ion from the Cu−Cu vector is the same for both cases; antiferromagnetic coupling is weakened, although the effect is more pronounced for the transoid geometry. Two different factors must be considered in order to explain this finding using the simple HTH model. Overlap of the d orbitals bearing the unpaired electrons with σ type MOs of the cyano bridge is certainly reduced in both distortions and, hence, the value of J is expected to decrease, but on the other hand, interaction with π type MOs should increase, changing the value of J in the opposite direction. The detailed balance between these two effects is, however, difficult to predict without performing accurate calculations.

Energetically, the transoid distortion is easily accessible, with deviations from the Cu−Cu vector down to 160° requiring less than 12 kJ/mol. The cisoid distortion is also feasible, with bending of the structure down to 170° requiring less than 12 kJ/mol. It is thus not surprising that the cyanide ions could loose their alignment with the Cu−Cu vector.

We also analyzed the effect of the distortion on the coupling constants for the cisoid and transoid distortions in model structure **3** (see **8**), with the cyanide anion bridging two axial positions (see Figure 4b).

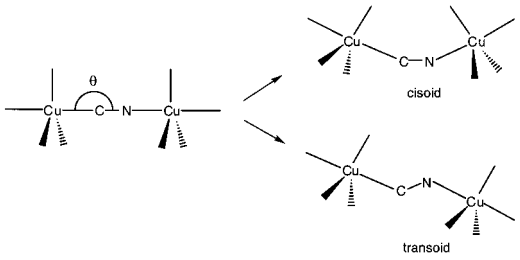

8

In this case the transoid distortion has the same effect as for model structure **2**; the antiferromagnetic coupling is strongly weakened. However, the cisoid distortion shows a surprising effect, moderately reinforcing the antiferromagnetic coupling. Although we have not been able to find a simple explanation for such a behavior, it is probably the subtle balance that involves interactions between the metal-centered d_{z^2}-type orbitals and the σ- and π-type MOs on the bridge. From the energetic point of view, both distortions are easily accessible in the crystal, requiring energies of the same order as those mentioned above for analogous distortions on model structure **2**, as found in many of the structures experimentally characterized in this work.

To check the applicability of our computational strategy to the evaluation of coupling constants in real compounds, we calculated J for three complete structures using the experimentally determined structural data. The position of the hydrogen atoms, which are not determined in the experimental structure, were guessed by optimizing them using molecular mechanics while fixing the position of all other atoms in the molecule.[37] As an example of a compound with an equatorial bridge (**2**) we have chosen $[Cu_2([14]\text{-}4,11\text{-}dieneN_4)_2CN](ClO_4)_3$. Its structure[33] is shown in Figure 5 , where one can notice that copper atoms are in a coordination environment that is slightly distorted toward the square pyramid ($\alpha = 93°$, $\beta = 112.7°$), while the CN bond is practically colinear with the Cu−Cu vector. The calculated J value is -2.4 cm^{-1}, which compares well with the experimental value,[38] -9.6 cm^{-1}.

As representative of compounds with an axial bridging mode (**3**), we have chosen $[Cu_2(tren)_2(CN)](PF_6)_2(ClO_4)\cdot 1/2\ KClO_4$ (see Figure 1 for the same cation structure) and $[Cu_2(tmpa)_2CN](ClO_4)_3$ (Figure 2). Both structures present a cisoid distortion at the bridge with average Cu−C−N angles of 162 and 174°, respectively. The calculated coupling constants are -109 and -54 cm^{-1}, which compare reasonably well with the experimental values of -158 and -100 cm^{-1}. The experimental and calculated data obtained for these two compounds are in fair agreement with the predicted variation of J with the Cu−C−N angle (Figure 4b); for the cisoid distortion, antiferromagnetic coupling is reinforced when departing from linearity. However, the change in the coupling constant is much larger than predicted for the model structure (Figure 4b). The different behavior found between our model compound and the complete structures can be understood by noting that in the first experimental structure the terminal N-donor atoms belong to an aliphatic amine (tren), whereas in the second structure we have aromatic N-donor atoms. In contrast, in our model calculations the same terminal ligands (NH_3) were used in both cases. In previous work on hydroxo-bridged dinuclear Cu(II) compounds,[18] we found that the strength of the antiferromagnetic coupling shows the same trend as the basicity of the terminal ligand; compounds with aliphatic amines as terminal ligands have stronger antiferromagnetic couplings than those with aromatic ones. This finding suggests that, in the present case, the reduction of the coupling constant from -109 to -54 cm^{-1} is not only due to the increase in the C−N−Cu angle, but also to the change in the terminal ligand. To evaluate the magnitude of these two contributions separately, we also calculated the value of J for a hypothetical $[Cu_2(tmpa)_2CN](ClO_4)_3$ molecule with a geometry in which the C−N−Cu is set to 162° while all other geometric parameters remain unchanged. The calculated value of J for this model, -78 cm^{-1}, indicates that the influence of the nature of the terminal ligands in this family of compounds is quite important. The calculated difference in J between the two experimental structures (from -109 to -54 cm^{-1}) can be roughly split in two similar contributions; 24 cm^{-1} can be attributed to the effect of the distortion, while 31 cm^{-1} are due to the effect of the basicity of the terminal ligands.

The calculations for complete structures show that the computational method employed throughout this work is able to give semiquantitative estimates of the coupling constant in complex structures. The results obtained for the three compounds also confirm that modeling this family of compounds using ammonia molecules as terminal ligands correctly describes the exchange coupling phenomenon. The replacement of the large terminal ligands by ammonia does not have a significant effect on the coupling constants for compounds with aliphatic amines as terminal ligands, a result that could be expected considering the similar properties of the nitrogen atom in NH_3 and NR_3 compounds. However, for a compound with aromatic N-donor atoms, one has to bear in mind that the absolute value of the

(37) Cerius^2 Program, Release 3.5; Molecular Simulations: San Diego, CA and Cambridge, UK, 1995.
(38) Duggan, D. M.; Jungst, R. G.; Mann, K. R.; Stucky, G. D.; Hendrickson, D. N. *J. Am. Chem. Soc.* **1974**, *96*, 3443.

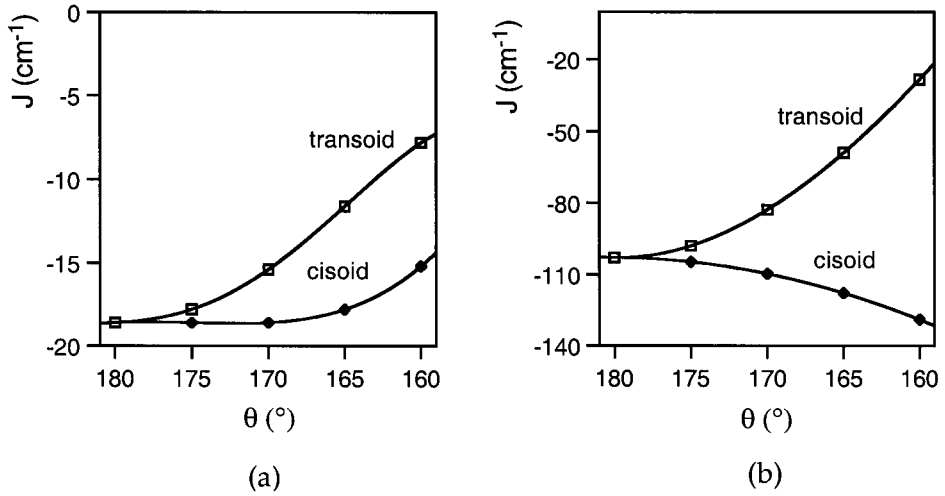

Figure 4. (a) Effect of the cisoid and transoid distortions (**7**) on the coupling constant *J* for model compound **2**. (b) Effect of the cisoid and transoid distortions (**8**) on the coupling constant *J* for model compound **3**.

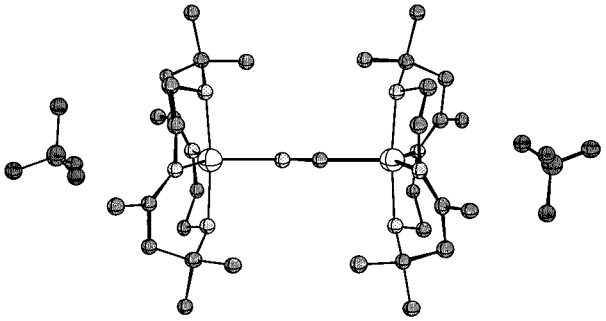

Figure 5. Structure of $[Cu_2([14]\text{-}4,11\text{-}dieneN_4)_2CN](ClO_4)_3$.[33]

calculated coupling constant will be about 30 cm^{-1} larger if the terminal ligands are replaced by ammonia molecules.

Theoretical Studies for Dinuclear Ni(II) Compounds. Examples of Ni(II) dinuclear compounds with cyano bridges are scarce. In the two known examples, the coordination sphere around the metal atoms is octahedral (**9**).

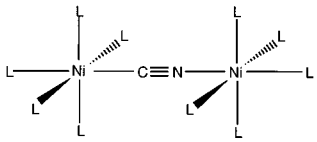

9

Since the same cation $[Ni_2(tetren)_2CN]^{3+}$ is present in both compounds, it is not surprising that both show antiferromagnetic coupling with nearly identical values of *J*, −24.5 and −24.8 cm^{-1}, respectively.

Following the same strategy as with the copper(II) compounds above, we adopted a model structure (**9**) in which all terminal ligands have been substituted by ammonia molecules. The structural parameters used in this model are perfect octahedral angles, $L_{eq}-Ni-L_{eq} = L_{eq}-Ni-L_{ax} = 90°$ and $L_{ax}-Ni-L_{ax} = 180°$, and average bond distances, $Ni-N_{term} = 2.14$ Å, Ni−C = Ni−N = 2.027 Å, and C−N = 1.164 Å. For the ammonia molecules, N−H = 1.015 Å and H−N−Ni = 109° were used. The calculated coupling constant for this model is −20.6 cm^{-1}, which is in excellent agreement with the experimental values found for both compounds.

As for the copper compounds studied previously, we evaluated the coupling constant for various distorted structures considering both cisoid and transoid distortion modes (**10**).

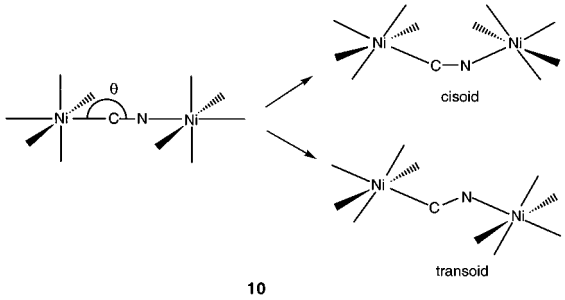

10

Figure 6a shows the calculated variation of the coupling constant with the Ni−N−C angle. For the cisoid distortion the coupling constant decreases rapidly, with a practically negligible coupling at angles smaller than 160°. The transoid distortion reinforces the antiferromagnetic coupling, which increases from −20.6 cm^{-1} for Ni−N−C = 180° to −27.0 cm^{-1} for Ni−N−C = 160°. This effect is just opposite to that observed for copper compounds, for which the transoid distortion weakens the antiferromagnetic coupling irrespective of the coordination position of the bridge. As previously found for copper compounds, the cisoid and transoid distortions of the bridging cyanide are energetically feasible for moderate values of the Ni−N−C angle (Figure 6b) and could be easily induced by packing forces in the crystal structure.

To check the validity of our computational model, we have also evaluated the coupling constant for the complete structure of $[Ni_2(tetren)_2CN]^{3+}$ on its two experimental geometries. In this case, we have not included the anions in the calculation since they do not present short distances to the metal centers. The position of the hydrogen atoms was guessed again by optimizing them using molecular mechanics.[37] The calculated coupling constants for both structures (see Figure 7) are −20.5 and −19.8 cm^{-1}, respectively, in excellent agreement with the experimental ones (−24.8 and −24.5 cm^{-1}), showing that the small structural differences between the two structures have a minor influence on the overall magnetic behavior.

Concluding Remarks

We report in this paper the synthesis, crystal structure, and investigation of the magnetic properties for several new cyano-bridged copper(II) and nickel(II) homodinuclear complexes. These species display a large range of compounds with distorted cyano bridges and various exchange coupling constants. It has

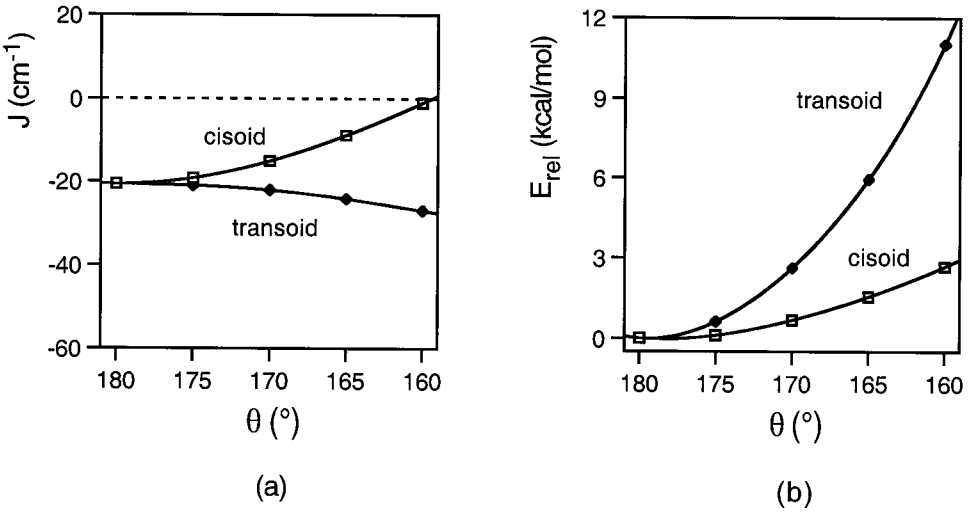

Figure 6. (a) Effect of the cisoid and transoid distortions (see **10**) on the coupling constant *J* for model structure **9**. (b) Relative energy of the broken-symmetry configuration for model compound **9** in the different steps of the cisoid and transoid distortions.

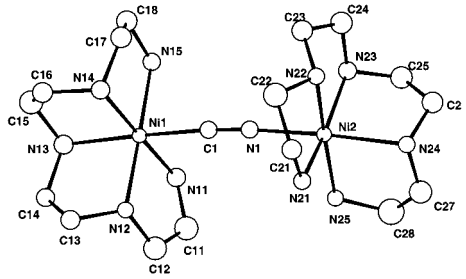

Figure 7. Structure of the $[Ni_2(tetren)_2CN]^{3+}$ cation in the compound $[Ni_2(tetren)_2CN][Cr(CN)_6]\cdot 5H_2O$.

been demonstrated that the ligands play an important role; for a given ligand, whatever the counteranion is, the geometry of the dinuclear complex and the exchange coupling parameter are nearly identical. The use of various ligands and the large variety of compounds allows the study of magnetostructural correlations. Our results show that the employed broken-symmetry DFT-based method provides good estimates of the *J* values even in systems with disymmetric bridges, like cyanide, that present a left−right localization of the SOMO orbitals. Comparison of the measured exchange coupling constants with those obtained from calculations allows the analysis of the influence of several structural factors (coordination position occupied by the bridging ligand, distortions of the coordination environment, nature of the terminal ligands, and the orientation of the cyanide ion relative to the M−M axis) on the coupling constant. For copper(II) complexes, with trigonal-bipyramidal coordination around the metal atoms, the magnitude of *J* is mainly influenced by the coordination position occupied by the bridging cyano ligand. In the case of cyanide ligands linking the two Cu atoms through their apical positions, the antiferromagnetic coupling is much more effective than when the cyanide ligand bridges two equatorial positions. For nickel(II) compounds, with octahedral environments around the metal atoms, the exchange coupling constant is only weakly affected by the experimentally observed deviations from the ideal coordination geometry. Deviation of the cyano bridge axis from the line joining both metal atoms, to give either a cisoid or a transoid geometry, has only a small effect on the coupling constant. The small energetic penalty calculated for these types of distortions is probably the reason they are frequently observed in experimental crystal structures.

Acknowledgment. The authors wish to thank Y. Dromzée for hepful discussion in the determination of X-ray structures. A.R.F. thanks CUR (Generalitat de Catalunya) for a doctoral grant. E.R. thanks the European Science Foundation (Molecular Magnets program) for a grant which made possible his stay in Paris. Financial support through the TMR program from the European Union (contract ERBFRMXCT98-0181) is acknowledged. Additional support came from Dirección General de Enseñanza Superior (DGES), through project number PB98-1166-C02-01, and from Comissió Interdepartamental per a la Recerca i la Innovació Tecnològica (CIRIT), through grant SGR99-0046. The computing resources at CESCA/CEPBA were generously made available through grants from CIRIT and Universitat de Barcelona.

Supporting Information Available: Crystal data, bond angles, anisotropic thermal parameters, and interatomic distances for compounds **A**−**F** (PDF). This material is available free of charge via the Internet at http://pubs.acs.org.

IC001420S